

Article

Analysis of the Spatio-Temporal Evolution of Dredging from Satellite Images: A Case Study in the Principality of Asturias (Spain)

Vanesa Mateo-Pérez ¹, Marina Corral-Bobadilla ^{2,*}, Francisco Ortega-Fernández ¹
and Vicente Rodríguez-Montequín ¹

¹ Project Engineering Department, University of Oviedo, 33004 Oviedo, Principality of Asturias, Spain; mateovanesa@uniovi.es (V.M.-P.); fdeasis@uniovi.es (F.O.-F.); montequi@uniovi.es (V.R.-M.)
² Department of Mechanical Engineering, University of La Rioja, 26004 Logroño, La Rioja, Spain
* Correspondence: marina.corral@unirioja.es; Tel.: +34-941-299-274

Abstract: One of the fundamental tasks in the maintenance of port operations is periodic dredging. These dredging operations facilitate the elimination of sediments that the coastal dynamics introduce. Dredging operations are increasingly restrictive and costly due to environmental requirements. Understanding the condition of the seabed before and after dredging is essential. In addition, determining how the seabed has behaved in recent years is important to consider when planning future dredging operations. In order to analyze the behavior of sediment transport and the changes to the seabed due to sedimentation, studies of littoral dynamics are conducted to model the deposition of sediments. Another methodology that could be used to analyze the real behavior of sediments would be to study and compare port bathymetries collected periodically. The problem with this methodology is that it requires numerous bathymetric surveys to produce a sufficiently significant analysis. This study provides an effective solution for obtaining a dense time series of bathymetry mapping using satellite data, and enables the past behavior of the seabed to be examined. The methodology proposed in this work uses Sentinel-2A (10 m resolution) satellite images to obtain historical bathymetric series by the development of a random forest algorithm. From these historical bathymetric series, it is possible to determine how the seabed has behaved and how the entry of sediments into the study area occurs. This methodology is applied in the Port of Luarca (Principality of Asturias), obtaining satellite images and extracting successive bathymetry mapping utilizing the random forest algorithm. This work reveals how once the dock was dredged, the sediments were redeposited and the seabed recovered its level prior to dredging in less than 2 months.

Keywords: Luarca port; random forest; dredging activities; sediment transport; satellite images



Citation: Mateo-Pérez, V.; Corral-Bobadilla, M.; Ortega-Fernández, F.; Rodríguez-Montequín, V. Analysis of the Spatio-Temporal Evolution of Dredging from Satellite Images: A Case Study in the Principality of Asturias (Spain). *J. Mar. Sci. Eng.* **2021**, *9*, 267.
<https://doi.org/10.3390/jmse9030267>

Academic Editor: Rodger Tomlinson

Received: 5 February 2021
Accepted: 25 February 2021
Published: 2 March 2021

Publisher's Note: MDPI stays neutral with regard to jurisdictional claims in published maps and institutional affiliations.



Copyright: © 2021 by the authors. Licensee MDPI, Basel, Switzerland. This article is an open access article distributed under the terms and conditions of the Creative Commons Attribution (CC BY) license (<https://creativecommons.org/licenses/by/4.0/>).

1. Introduction

Dredging activities are commonly used in coastal areas to maintain the designed depth of navigation channels or basins and to remove deposited sediments. These activities include not only the processes of removing sediment from the bottom, but also their subsequent transport to another location. Dredging of ports improves access and exit conditions for cargo and passenger ships [1,2]. This is important for marine safety, removing sediment that has accumulated in channels in order to maintain the designed depths of the existing facilities [3,4]. However, despite its importance in maritime works and its effect on economic and social development, and the current advances in dredging techniques, the siltation of ports continues to be one of the least understood branches of coastal engineering. It is of great importance to ports, in maintaining and improving its depth and, also, in developing new facilities or creating new ports [5]. Thus, it is particularly important to study the sedimentation that takes place in the basins and entrance channels of ports. Excessive sedimentation can impair the functioning of the port and lead to a decrease in

economic activities [6–8]. The construction of dikes and other coastal protection works have a great influence on hydrodynamic forces and movement of sediment in the offshore area [9]. Hydrodynamic and sedimentary conditions can cause sedimentation of the port channel, which must be removed by maintenance dredging [10].

The Port of Luarca is located in the Principality of Asturias and is one of the most important ports in northern Spain. In recent years there have been significant changes in the marine dynamics of the port, as well as in the erosion–sedimentation processes that operate there. To maintain navigation, dredging is undertaken once a year. Technical specifications include the estimation of siltation volume, location, duration and phases of dredging works to be performed, the dredging method and the location of suitable sediment dumping locations that will not affect the environment adversely [11]. At Luarca, sandy bottoms prevail, although several areas are presently covered by mud [12]. The purpose of dredging the dock area is to guarantee the functionality of the port, which is conditioned by the depth of the dock. The location of the Port of Luarca at the mouth of the Rio Negro favors the accumulation of sedimentary materials of fluvial origin. The dock's location forestalls the tidal dynamics that are necessary to wash away the deposited sediments. For this reason, periodic dredging is necessary to maintain the dock. This enables optimal levels of use of the different port areas to be achieved. Throughout its operational life, the port has faced significant sedimentation problems and a consequent decrease in the depth of the draft in its entrance channel. The problem of sedimentation is increasing due to the environmental problems that are associated with dredging and the restrictive regulations imposed as a result. This sedimentation problem may be related to the positioning and layout of the port basin and its entry location [13,14]. Due to high sedimentation rates, the basin and entrance channel of the Port of Luarca must be dredged regularly for the port to continue its operation.

Many different methodologies have been used in an effort to understand the behavior of sediments. These have ranged from the use of probabilistic design methods [15–18] to direct numerical simulations [19–21]. Direct numerical simulations provide a rough understanding of the behavior of sediments. However, it is a costly methodology, because it requires the survey of the entire area in order to understand its 3D geometry. Another technique that could be used to study the behavior of sediments is to conduct an analysis of the bathymetries that were obtained in the study area. If the evolution of the seabed is known, it is possible to know where the sediment deposits are produced and their sedimentation rate. This technique would also help to determine the need to undertake dredging, as well as its periodicity. The main limitation when analyzing the behavior of the seabed is the availability of bathymetries. Bathymetries are normally conducted before and after dredging, but not frequently enough to understand the evolution of the seabed, due to their high cost and the difficulty of carrying them out. This clearly limits their use in analyzing the behavior of the seabed. Therefore, for this purpose, bathymetries are obtained from satellite images using the simplest techniques that offer a high level of precision. In addition, the techniques must be applicable in areas of turbid and shallow water and provide rapidity and flexibility of use.

Conventional bathymetric methods usually provide depth profiles or point measurements of acceptable accuracy. However, their use is costly and inefficient. Bathymetric estimation can be improved by combining echo sounding and satellite data. Remote sensing technology is used in many topographical studies. This is very useful for situations in which the depths of water are required on temporal and spatial scales, but are difficult to obtain [22–25]. Simple methods that use optical images in estimating depths are used by some investigator methods, as well as linear regression algorithms to estimate the depth of water [26]. In recent years, the use of machine learning techniques and optical sensors to estimate bathymetries has gained popularity. This can be attributed to advances in the development of algorithms, as well as greater availability of data and new satellites. Many authors have sought to determine the depths of water depths from optical sensors and the use of regression models that were derived from machine learning techniques [27–32]. The

random forest algorithm was used in this study to obtain the bathymetries. This algorithm has a number of advantages, including, low-cost, simplicity, time-effectiveness, and its wide-coverage for shallow water. Thus, the random forest algorithm has been found to be applicable to construct regression models that rely on bathymetry data from satellite images [33–41].

Many studies have concentrated on migration of sediments over the long term and how this affects water quality and the ecosystem condition. They model movement of material that is removed during the dredging operation [42]. However, optimizing the dredging operation has not been proposed. The main objective of this work is to determine if the behavior of sedimentation differs with the depth of dredging. In other words, is there a stable mean depth outside of which erosion and sedimentation occur more quickly? This is possible due to the capacity of the methodology, which enables data from the past with a frequency of 1–2 months to be analyzed. This provides great information of the seabed's behavior.

2. Study Site

The Port of Luarca is situated in northwestern Spain on the coast of the Cantabrian Sea at a longitude of 6°32'1" W and a latitude of 43°32'45" N (Figure 1a). Luarca has been associated with maritime activity since it began as a fishing enclave in the 10th century. Several changes have occurred throughout past years in Luarca Port. In 1910, the Canouco dike (Figure 1b), 40 m in length, was built to shelter the outer basin of the port. In 1940 a new dike, the La Encoronada dike, was built (Figure 1b), 124 m in length on the western side [43]. It is necessary to conduct dredging of the dock annually. The lack of draft means that the boats cannot enter the port, as many currents are generated in the entrance channel. Thus, navigation in this area is endangered by the risk that the boats will be stranded, especially during storms. The port is used generally by small boats. Thus, the minimum drafts in the navigation channel range from 2 to 3 m, with an average tidal run of 2 m. The draft in the docking area is somewhat less—2 m. Although dredging is conducted in the inlet channels, it also affects the inner basin. Of the two areas, it is the inner basin that receives the most interventions and is most limited due to draft. Nalona, a dredger boat (Suction Hopper Dredger, IMO 9047453) [44], has been used to dredge the bed surrounding the port. After the sand and mud have been collected from the bottom of the Port of Luarca, the sand is deposited in the area of Punta Muyeres, in front of the third beach of the village, in an effort to renew this area. However, it is not very clear whether this discharge location benefits the port, since a large amount of the sand that is dumped there will be moved by the currents and re-enter the dikes. The mud, on the other hand, is deposited at another location that is farther from the beaches.

The dates on which the dredging is carried out in the inner basin are provided by the Port Service of the Principality of Asturias. Dredging operations were carried out in 2017 and 2018. In 2017, the dredging began in October, but was stopped because of a problem with the dredge. It resumed in November and ended in December, 2017. In 2018, dredging began on November 15 and continued until the end of the year. In 2019, the inlet channel was dredged, but little work was done in the inner basin.

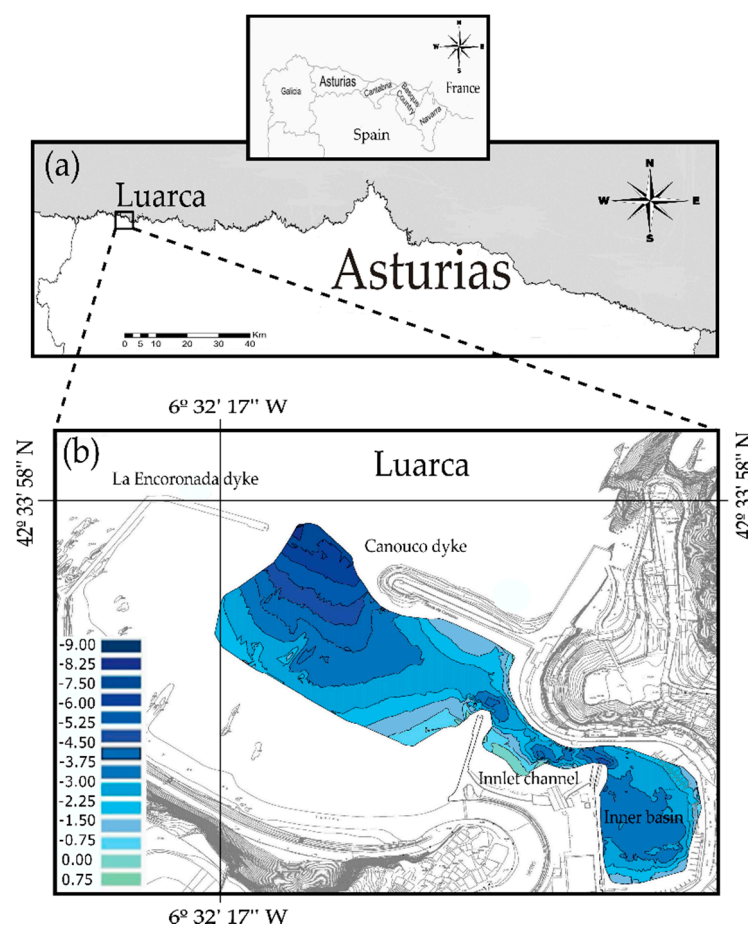


Figure 1. The Port of Luarca: (a) position of the port on the Cantabrian Sea coast; (b) the study site location.

3. Data and Methodology

3.1. Data In Situ Measurements and Satellite Data

Field measurements are generally necessary to study the sedimentation in the port, including the hydrodynamic parameters of the area, in this case only bathymetries will be used as field measurements, and these bathymetries are provided annually by the Port Service of the Principality Asturias. The bathymetries were conducted with the use of a Navisound 210 single beam echo sounder, with a 1 cm vertical resolution and dual frequency (Reson, Inc.: Slangerup, Denmark). The specifications of echo sounder Navisound 210 are shown in Table 1.

Table 1. Characteristics of echo sounder Navisound 210.

Navisound 210/400	Specifications
Frequency	190–235 kHz
Potency of transmission	300 W
Impedance	100 Ohm
Echo approval length	100 μs–210 kHz
Depth range	0.5–100/400/1200 m depending on the frequency
Resolution	1 cm
Accuracy	1 cm at 210 kHz (1 σ) assuming correct sound velocity, transducer depth etc.

The study’s echo sounding data for Luarca were determined, on 28 June 2016, 10 May 2018 and 28 May 2019. For the present work, XY positions from the survey data were

projected using UTM Zone 30N. As they are usually costly, they are normally used only for specific dates. The satellite Sentinel-2 provided the data with which to predict the bathymetry of the water depth at the port (Table 2).

Table 2. Dates of acquisition of bathymetries.

		Year		
2017	2018	2019	2020	
		05/01/2019	25/01/2020	
	24/02/2018	24/02/2019	19/02/2020	
	16/03/2018		10/03/2020	
	10/04/2018	20/04/2019		
		30/05/2019		
	24/06/2018	14/06/2019		
04/07/2017	29/07/2018	24/07/2019		
13/08/2017	18/08/2018	23/08/2019		
02/09/2017	02/09/2018	12/09/2019		
02/10/2017	02/10/2018	22/10/2019		
21/11/2017	16/11/2018	21/11/2019		
21/12/2017	31/12/2018			

3.2. Methodology

The process to obtain the bathymetries is shown schematically in Figure 2.

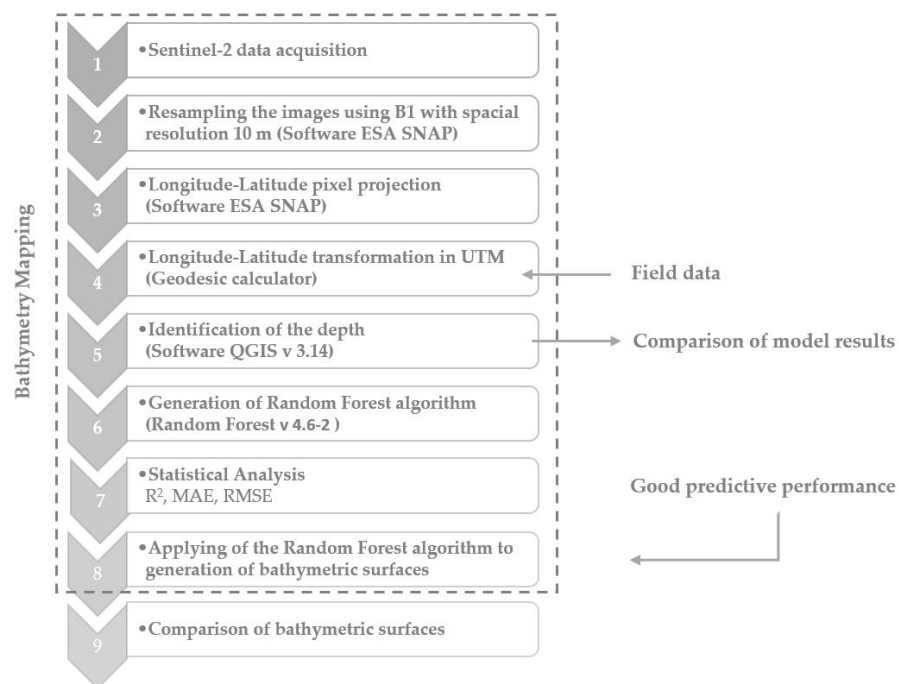


Figure 2. Methodological workflow for development of bathymetric maps.

3.2.1. Processing Satellite Images

The processing step concerns using Sentinel-2A data as vector of variables for training and fitting of the random forest model (Figure 2). Sentinel-2A satellite data was retrieved from ESA Copernicus Open Access Hub. SNAP (Sentinel Application Platform) software was used to visualize and preprocess Sentinel-2A data (10 m resolution) [45]. The data from the Sentinel-2A satellite reflectance bands (B1, B2, B3, B4, B5, B6, B7, B8, B8A, B9, B11, and B12) were used to predict the depth of the water at the study port. All spectral bands in the Sentinel-2A images were resampled to achieve a resolution of 10 m using the SNAP S2 Resampling Processor [15,46,47]. As a result, a dataset without georeferencing

was obtained, and to determine the positioning of the reference points, the geographical location of each point was defined by its longitude and latitude using the SNAP program. Then, using the WGS84 ellipsoid, a coordinate projection was created in order to obtain the coordinates in ETRS89 [48]. This system was also used to project the positions that the echo sounder provides. The ellipsoid projections had an average position error of 1 cm. The data that was obtained was compared to the bathymetry that had been projected. To accomplish this, a geodesic calculator was used to project the coordinates. This enabled the authors to obtain the data for bands that are associated with UTM x-y coordinates. The random forest algorithm was used to assign the z coordinate. From these points and using the QGIS software (version 3.14), the surface was obtained by digital models of the TIN (Triangulated Irregular Network) terrain type. Triangulation was undertaken using linear interpolation [49]. The error that this process involved was small due to the absence of any great irregularities in the smooth surfaces of the seabed. The port's zero serves as the reference point for the z coordinates. The former is the minimum measured level of the surface of the water during the highest low tide in the last 15 years. Pixels were assigned dimensions on the basis of their x-y locations.

3.2.2. The Random Forest Algorithm

The random forest algorithm [50] facilitates classification and regression by use of a randomized subset of predictors that enable it to create a variety of classification trees [51]. Many of the trees start as bootstrapped training data samples. A random subset of predictor variables (z coordinate) is used at each fork in the process. This causes each tree to be different. Although each tree is a poor predictor, each pair of them provides a different response. This aggregates the predictions of uncorrelated trees, reducing prediction variance and increasing accuracy [52–54]. This work involved 100 trees and 13 variables (Sentinel-2A satellite bands B1, B2, B3, B4, B5, B6, B7, B8, B8A, B9, B11, and B12, and tidal). The default value was adopted as the minimum size of nodes. The random forest algorithm for prediction of bathymetry was provided by the Random Forest (v 4.6-2) R package [55].

3.2.3. Training and Testing Dataset

In order to evaluate the accuracy of the model, the dataset that was obtained from Sentinel-2 was divided into two groups. Training the random forest algorithm required 80% of the dataset (1593 data points), and testing the model used the remaining 20% (388 data points). Data from echo sounding measurements were used to calibrate the model without any kind of elaboration [56]. To test the model, the data obtained with the model were compared with field measurements for 20% of the points. As the tide affected the depth measurement results, the measured depths were the mean sea levels (MSL) that served as references. This was accomplished by deducting the measured depth during high tide from the MSL. The tidal data were provided by the nearest tidal station [34].

Finally, in order to determine the accuracy of the model's estimates of depth, satellite derived bathymetry maps were compared with that of the field measurements obtained by using the echo sounder. The residual statistic between the satellite derived depth ($Z_{satellite}$) and the echo sounding measurements ($Z_{echo-sounder}$) were reported along three metrics. They were the mean absolute error (MAE), the root mean squared error (RMSE) and the correlation coefficient (adjusted R^2). They are calculated by the equations below.

$$MAE = \frac{1}{n} \sum_{i=1}^n |Z_{Satellite} - Z_{echo-sounder}|$$

$$RMSE = \sqrt{\frac{1}{n} \sum_{i=1}^n (Z_{Satellite} - Z_{echo-sounder})^2}$$

$$R^2 = \frac{\sum_{i=1}^n (Z_{echo-sounder} - \overline{Z_{echo-sounder}}) (Z_{Satellite} - \overline{Z_{Satellite}})}{\sqrt{\sum_{i=1}^n (Z_{echo-sounder} - \overline{Z_{echo-sounder}})^2 \sum_{i=1}^n (Z_{Satellite} - \overline{Z_{Satellite}})^2}}$$

where $Z_{Satellite}$ are the depths that the random forest methodology predicted from Sentinel-2 images. $Z_{echo-sounder}$ denote the in situ echo sounding depths and n is the number of data.

4. Results

The random forest algorithm achieved a good predictive performance, with an MAE of 0.37, an RMSE of 0.47 and an R^2 of 0.974. The testing data set results appear in Table 3.

Table 3. Error statistics reported in meters produced by the random forest algorithm.

Algorithm	MAE (m)	RMSE (m)	R^2
Random forest	0.37	0.47	0.974

Figure 3 provides a histogram of the relationship between mean absolute error (MAE) and the depth of the port of Luarca that was obtained by the random forest algorithm. As can be seen in Figure 3, the maximum error (60 cm) occurred between -6 and -8 m and the minimum (24 cm) occurred at -10 m. This error is acceptable for the purpose of this study, which is to analyze the behavior of the seabed with respect to time.

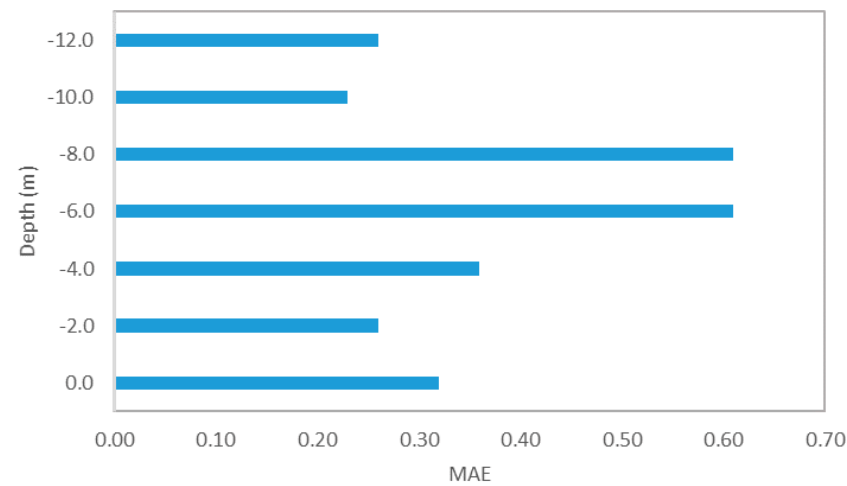


Figure 3. Variation of MAE errors versus depth (m).

As an example of the results that were obtained, the bathymetries before and after the 2017 dredging are represented in 3D and 2D (Figures 4 and 5). Figure 4 represents the 3D evolution of the seabed for 21/11/17 (Figure 4a), 21/12/17 (Figure 4b) and 24/02/18 (Figure 4c). These show that the elevation of the seabed was maintained in Figure 4a,b, but had declined in Figure 4c due to dredging.

Figure 5 represents one of the dredging episodes by a series of bathymetries that were analyzed in the plane and profile view. These indicate the effect of the dredging that was undertaken. First, when dredging is carried out, there is a decrease in the elevation of the basin and the inlet channel (Figure 5a,c). The elevation recovers when the dredging stops (Figure 5b,d). This effect is seen in both the inner dock (section AA') and in the inlet channel (section BB'). In both representations (Figures 4 and 5), the areas of greatest variation are the inner basin and the inlet channel. These are the areas where dredging takes place. Additionally, in Figures 4 and 5, the areas in which the greatest changes occur are in the lower right corner (inner dock area and inlet channel) and in the upper left corner that coincides with the beach area. Both are areas that undergo many changes in topography due to coastal dynamics.

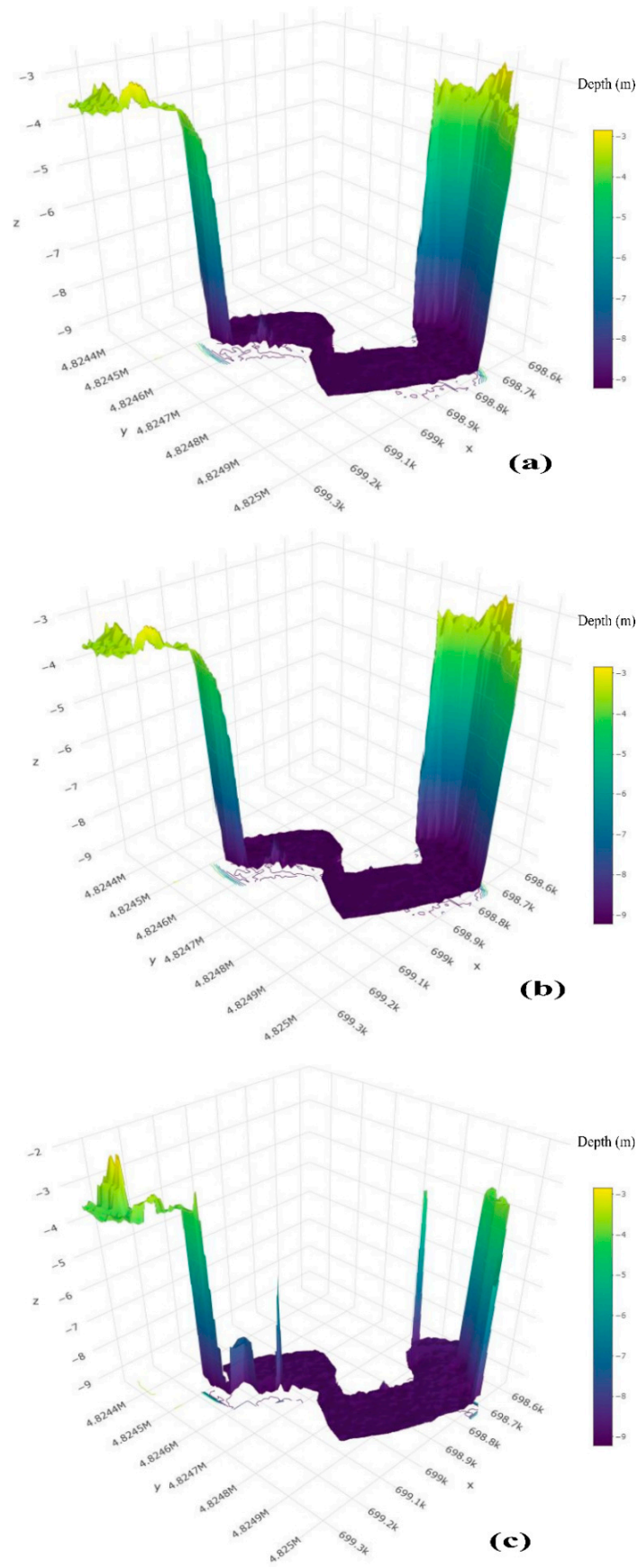


Figure 4. 3D bathymetries. Dates: (a) 21/11/17, (b) 21/12/17 and (c) 24/02/18.

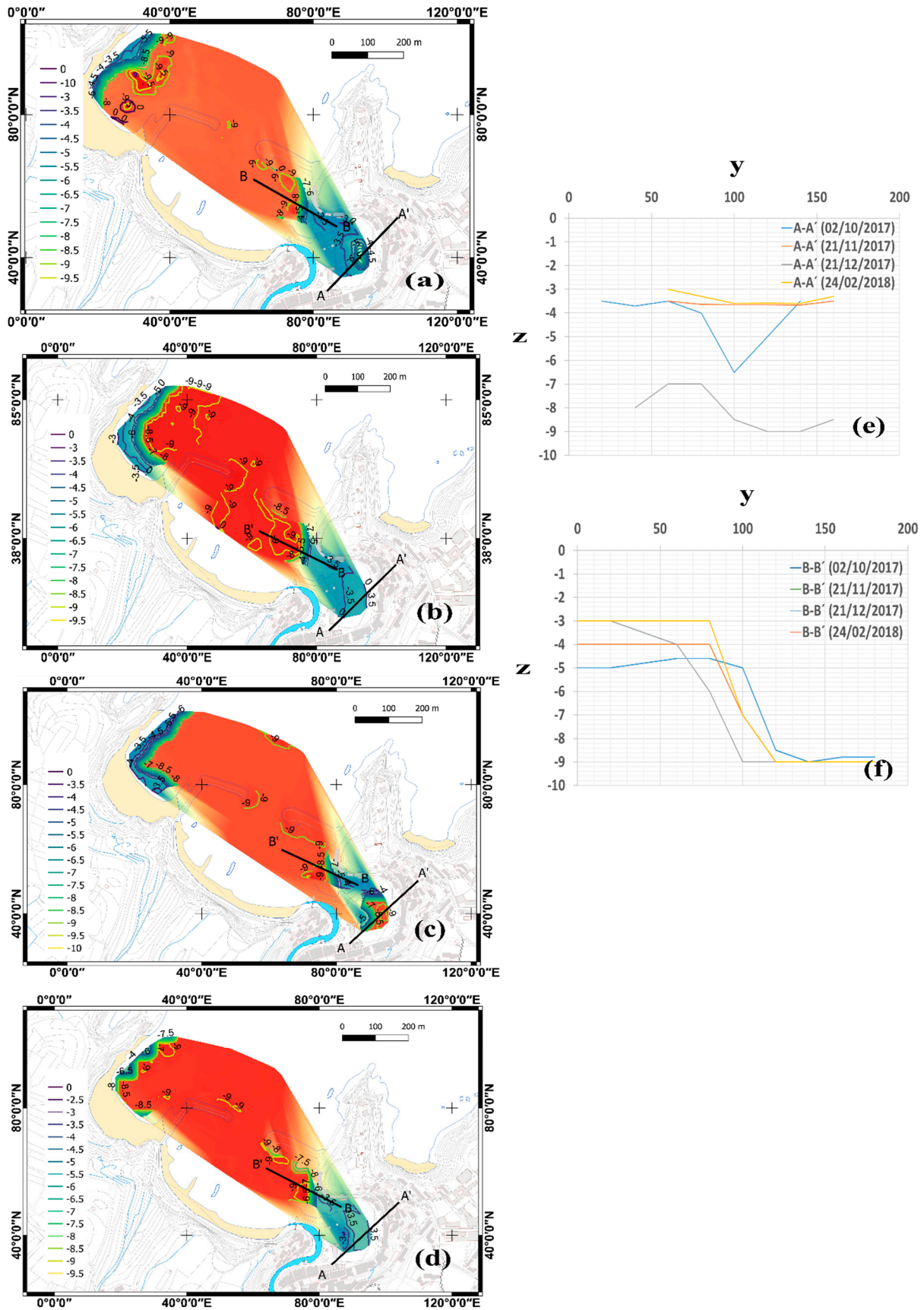


Figure 5. A representation of the behavior of the interior basin the dredging on: (a) 02/10/17, (b) 21/11/17, (c) 21/12/17 and (d) 24/02/18; and cross-sectional profile (e) AA' of the inner dock, and (f) BB' of the inlet channel.

After the surfaces were generated, they were compared—bathymetry to bathymetry—sequentially in time in order to examine the erosion and the sedimentation that occurred. This is done by comparing the difference between the surfaces that are generated for each bathymetry that is analyzed. To study the evolution of sediment in the basin of the Port of Luarca, the surfaces for each of the bathymetries obtained from the use of satellite images and the random forest algorithm were generated. Once the surfaces were obtained, the differences between them were analyzed. Comparing these surfaces, the erosion and sedimentation volumes were obtained.

In the results that appear in Table 4, the first and second columns provide the dates on which the bathymetry comparison was made. The third column provides the duration or time interval between bathymetries. The fourth column shows the volume of the main activity (erosion or sedimentation) by day that was generated. The fifth column shows the erosion or decrease in volume between the first and second bathymetry (sediment that exited the basin area), whereas the sixth column provides the sedimentation or volume increase between the first and second bathymetry (sediment that entered the basin area). The seventh column provides the total value of the difference between sedimentation and erosion. The eighth column shows an error assessment analysis in terms of volume change. The last column of the table shows when the dredging was undertaken.

Table 4. Evolution of sedimentation in the Port of Luarca.

Starting Date	Finishing Date	Time (Day)	Rate (m ³ /Day)	Erosion Volume (m ³)	Sedimentation Volume (m ³)	Total (m ³)	Total Error (m ³)	
04/07/2017	13/08/2017	40	29.26	74.88	1245.11	1170.23	±110.31	
13/08/2017	02/09/2017	20	402.46	0.00	8049.16	8049.16	±878.69	
02/09/2017	02/10/2017	30	−548.80	16,463.97	0.00	−16,463.97	±1571.27	Start Dredge
02/10/2017	21/11/2017	50	99.10	263.30	5218.13	4954.82	±337.91	Stop Dredge
21/11/2017	21/12/2017	30	−1231.98	37,030.08	70.80	−36,959.29	±3343.98	Dredge
21/12/2017	24/02/2018	65	589.90	80.24	38,423.49	38,343.25	±3502.55	
24/02/2018	16/03/2018	20	−310.62	6215.43	2.93	−6212.50	±432.64	
16/03/2018	10/04/2018	25	169.35	24.94	4258.79	4233.86	±287.25	
10/04/2018	20/05/2018	40	120.86	0.00	4834.25	4834.25	±370.84	
20/05/2018	24/06/2018	35	19.80	518.85	1211.81	692.96	±68.85	
24/06/2018	29/07/2018	35	−48.44	2084.56	389.03	−1695.53	±165.76	
29/07/2018	18/08/2018	20	46.14	159.70	1082.48	922.78	±89.14	
18/08/2018	02/09/2018	15	−104.60	1668.90	99.85	−1569.05	±150.34	
02/09/2018	02/10/2018	30	−57.35	1792.12	71.55	−1720.57	±157.61	
02/10/2018	16/11/2018	45	14.65	532.99	1192.31	659.32	±59.24	
16/11/2018	31/12/2018	45	−597.85	26,910.49	7.34	−26,903.15	±2752.28	Dredge
31/12/2018	05/01/2019	5	3556.35	12.93	17,794.68	17,781.76	±1655.70	
05/01/2019	24/02/2019	50	239.28	33.00	11,997.16	11,964.16	±832.46	
24/02/2019	26/03/2019	30	−1.03	438.94	408.12	−30.82	±3.04	
26/03/2019	20/04/2019	25	697.02	0.00	17,425.54	17,425.54	±1971.12	
20/04/2019	05/05/2019	15	−592.93	8893.90	0.00	−8893.90	±1227.16	
05/05/2019	30/05/2019	25	−311.02	7775.56	0.00	−7775.56	±894.89	
30/05/2019	14/06/2019	15	594.02	0.00	8910.36	8910.36	±1046.90	
14/06/2019	24/07/2019	40	−236.76	9470.57	0.00	−9470.57	±1101.37	
24/07/2019	23/08/2019	30	−20.47	697.96	83.96	−614.01	±60.14	
23/08/2019	12/09/2019	20	2.99	267.98	327.82	59.84	±5.82	
12/09/2019	22/10/2019	40	−39.67	1632.29	45.49	−1586.80	±150.54	
22/10/2019	21/11/2019	30	−66.90	2007.10	0.00	−2007.10	±181.28	
21/11/2019	26/12/2019	35	−132.28	4742.30	112.66	−4629.64	±319.05	
26/12/2019	25/01/2020	30	287.98	0.00	8639.33	8639.33	±630.13	
25/01/2020	19/02/2020	25	46.14	120.48	1273.91	1153.43	±115.83	
19/02/2020	10/03/2020	20	−118.73	2374.51	0.00	−2374.51	±234.22	
10/03/2020	04/04/2020	25	52.91	137.30	1459.93	1322.63	±128.26	

Table 4 shows the increase in the rate of sedimentation, notably after the dredging work of $589.90 \text{ m}^3/\text{day}$ after the 2017 dredging and $3556.50 \text{ m}^3/\text{day}$ after the 2018 dredging. In the 2017 dredging, $16,463.97 \text{ m}^3$ were extracted and, after stopping the work, the amount of sediment that was released was $37,030.08 \text{ m}^3$. In the following period, $38,423.49 \text{ m}^3$ sediment were extracted, which is more than was dredged in the previous month. In fact, 5218.13 m^3 of sedimentation occurred in the breakdown period.

In the 2018 dredging, $26,910.49 \text{ m}^3$ were extracted, $17,794.68 \text{ m}^3$ of which were extracted in just 5 days. In order to analyze more precisely the operation of the inner basin of the Port of Luarca, the variations in elevation during the dredging work were represented, as well as after the completion of the dredging in 2017 and 2018 (Figures 6 and 7).

In Figure 6a it can be seen that, after stopping at the end of October 2017, the areas where the dredging was conducted during the September–October period were immediately filled with sand again. The same is seen in Figure 6b,c. It can be seen that the elevation dropped substantially while the dredging was being conducted (Figure 6b), but had recovered in the next bathymetry (Figure 6c) to the original elevation.

The bathymetries in Figure 6 also show how dredging was carried out. In the specific way that the suction dredger is used, it acts on an area of the surface, substantially lowering the elevation. Later, the coastal dynamics fill these areas, thereby lowering the level of the entire dock. In reality, this low point is not filled with the adjacent material in the basin itself. Instead, it is filled by external sediment. Thus, the dredging effect does not last very long. This same analysis was conducted for the 2018 dredging (Figure 7).

Figure 7 represents the variation of the bathymetries of the bottom in the Port of Luarca. Figure 7a shows that the bottom falls due to the dredging carried out, achieving a total decrease in height of 5.5 m at the lowest point. In the bathymetry of Figure 7b, practically everything that has been extracted by dredging has been replaced, increasing the elevation by 5 m where the increase had been greatest. In this case, it is important to note that the variation that is reflected in the bathymetry occurs only on 5 days. In Figure 7c it can be seen that the bottom continued to recover the sediments throughout the following months until it had returned to its original level.

To analyze the behavior of the basin bottom elevation for periods not analyzed above, the average depth of the basin bottom of the port was analyzed (Figure 8).

Figure 8 shows the average depth of the bottom at the dock in the Port of Luarca. It can be seen that the dredging was done at the end of 2017. It began in October 2017, but became impossible to continue during November due to problems with the dredge. Thus, this dredging ended in December 2017. Figure 8 shows that the recovery of elevation was almost immediate. Additionally, as can be seen in Figure 8, the same phenomenon occurred in 2018, with dredging concluding at the end of the year, but the port's equilibrium level recovering in the beginning of 2019.

Aside from the phenomena of dredging and rapid recovery of the average level, the behavior of the bottom was quite stable, except for some sediment entry points. It is important to note that even these sediment entry peaks are regulated and without external intervention, with the bottom returning to its average level. In this case, a mean elevation or equilibrium profile of between -3 and -4 m was verified.

To determine why there are points that experienced an entry of sand in the docking area that exceeded the balance level, the wave height was analyzed (Figure 9). The data was supplied by a multiparametric buoy that was deployed in the area surrounding Gijón Harbor [42].

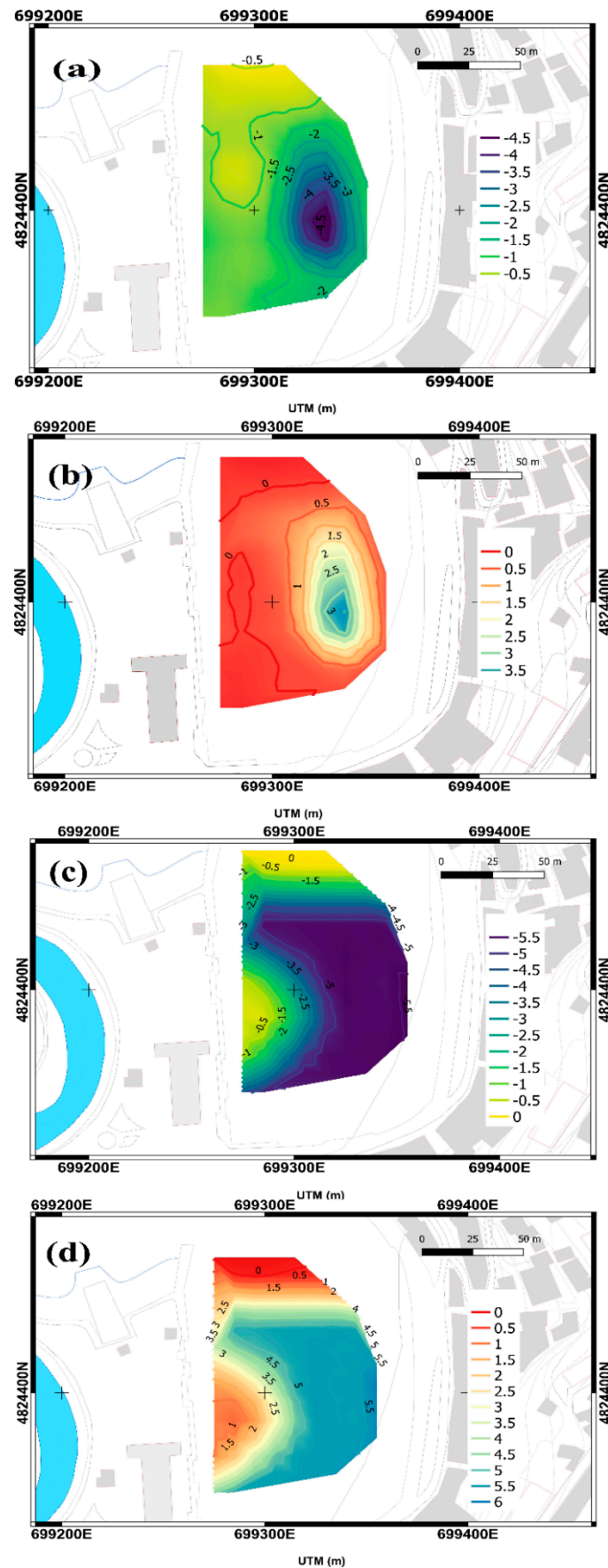


Figure 6. Difference in elevation of the bathymetries in the Port of Luarca between (a) 02/09/17 and 20/10/17, (b) 02/10/17 and 02/11/17, (c) 21/11/17 and 21/12/17, and (d) 21/12/17 and 24/02/18.

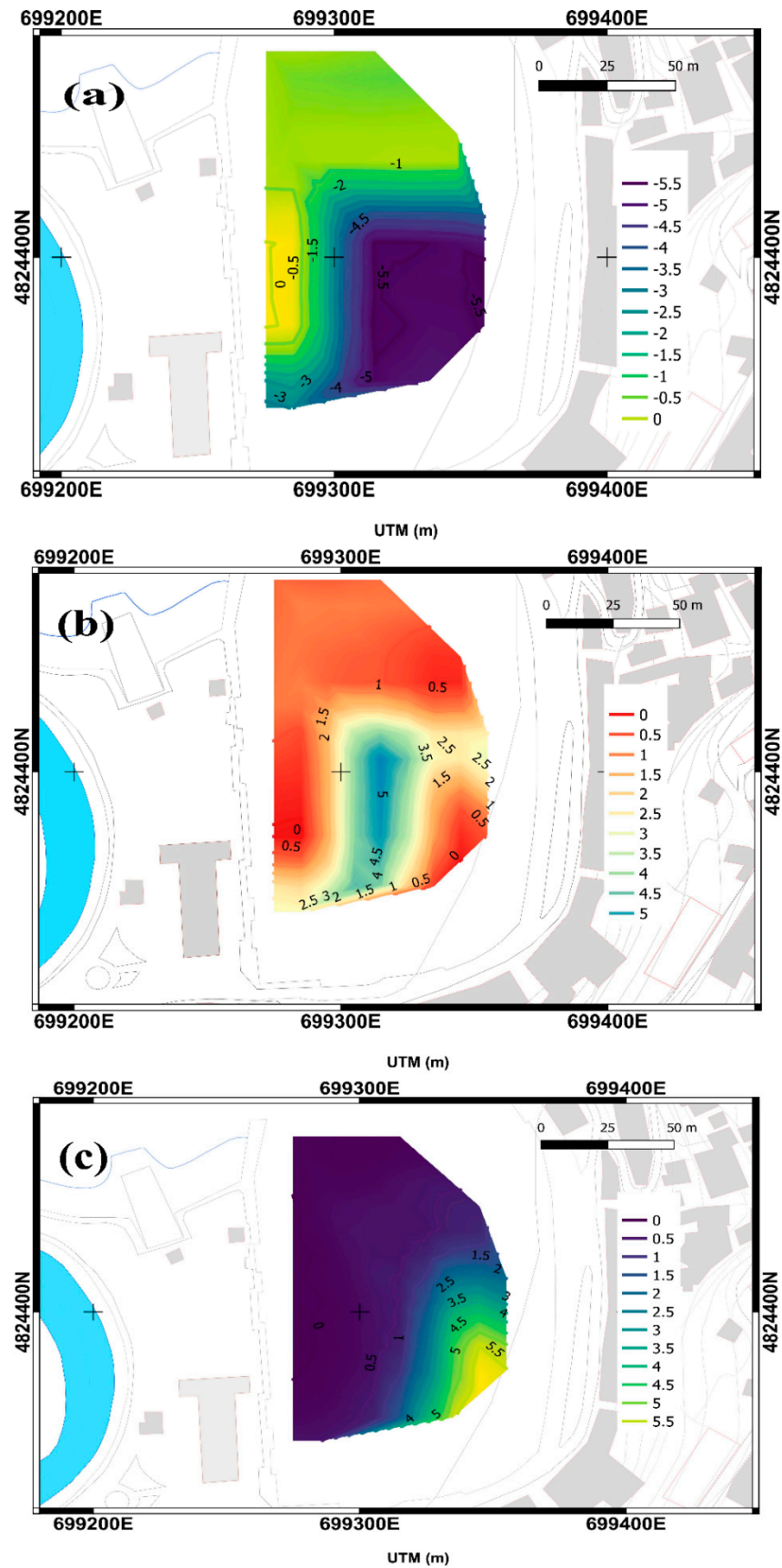


Figure 7. Difference in elevation of the bathymetries in the Port of Luarca between (a) 16/11/18 and 31/12/18, (b) 31/12/18 and 05/01/19, and (c) 05/01/19 and 24/02/19.

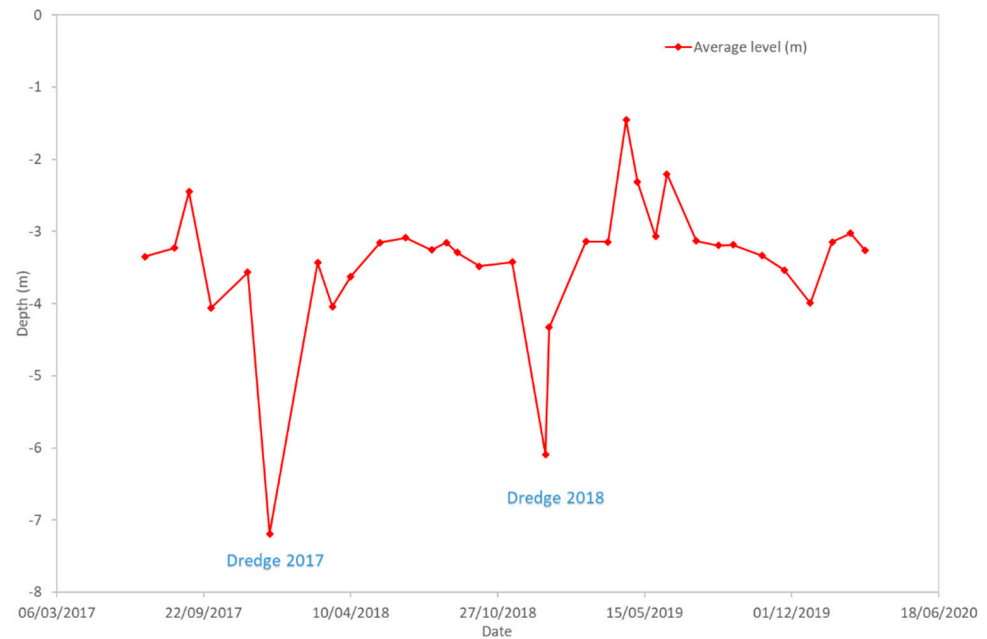


Figure 8. Average depth of the bottom of the dock in the Port of Luarca.

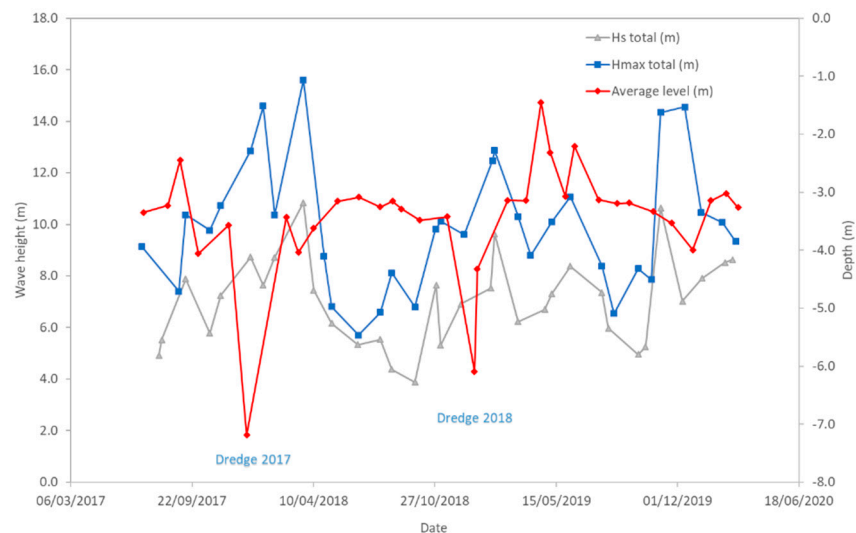


Figure 9. The effect of the wave height (H) on the average level of the dock in the Port of Luarca.

Figure 9 shows the effect of waves on the average level of the dock in the Port of Luarca. It shows that there were three important wave points. The one that followed the 2017 dredging produced a slight rebound of the mean elevation of the basin. The second important wave point occurred after the second dredging, which generated a more significant increase in the mean elevation. Finally, the third wave point of importance marked the end of the period that was being studied. However, as at the end of 2019, no dredging was conducted, and the elevation was stable. Thus, the impact of the waves was barely noticed. There appeared to be a relationship between the oscillation of the seabed levels and the waves. However, in order to confirm this, it would be necessary to carry out a more detailed study to measure the waves in the port itself.

The sand entry peaks, but much less pronounced, correspond to storms. As can be seen in Figure 9, these sand entries also disappeared, recovering the equilibrium point. The Negro River is another entry point for sedimentation. This river is a short coastal river in the north of Spain. It runs through the western part of the Asturias and flows into the

Cantabrian Sea, on the beach of Luearca. There is an Automatic Hydrological Information System (SAIH) in this river. It was from this control point that the data were obtained [57].

To study the possible influence of the river on the contribution of sediments in the basin, the mean level of the basin was compared to the level of the river (Figure 10).

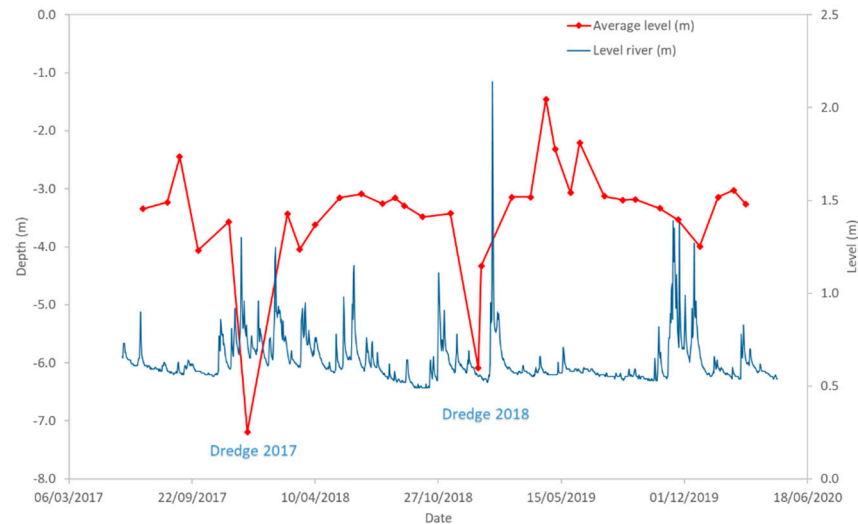


Figure 10. Effect of the Negro River on the average level of the dock in the Port of Luearca.

Figure 10 shows that a significant elevation of the river level does not imply an entry of sediments. The highest elevation of the Negro river level occurred on 01/23/2019 and the lowest level of the dock was reached at the end of March 2019 and ended 1 month later.

5. Conclusions and Discussion

One of the most important tasks for port maintenance is dredging. The objective of this is to maintain the draft within values that permit vessel to enter and exit from the port. This work examined how the bottom of the interior basin of the Port of Luearca behaves during dredging and subsequent periods by analyzing the data of 4 years. In order to study the variations in the surface of the seafloor, it was necessary to obtain bathymetries of it. Bathymetries are conducted annually in this port, but there is insufficient data for an analysis of these variations. These bathymetries must include the depth of the seabed at several points that are spaced appropriately, in addition to the planimetric position of these points and measurements of the variations in the mean level of the surface of the sea. Due to the ongoing modeling of seafloor level and the numerous bathymetric survey data sets and use of remote sensing technology, it is possible to estimate the volume of sedimentation and, therefore, how much sediment has accumulated in a navigation channel. The layers of sediment to remove in maintenance dredging are generally not very thick. Thus, in order to avoid unnecessary dredging-related expense, seafloor levels should be determined and modeled accurately.

The purpose of his study was to find a practicable method to obtain a dense time series of bathymetries using satellite data. This would enable the past behavior of the seabed to be analyzed. Bathymetries could also be obtained by continuous conventional measurements using echo sounders. However, there are issues of accuracy and precision at present. Additionally, shallow coastal waters are difficult to access. Hence, it is not possible at present to analyze past behavior. It is also necessary to wait until a sufficiently large data series can be obtained before the behavior of the seabed can be described with certainty.

To facilitate this work, several bathymetries were obtained on different dates from Sentinel-2 satellite images and the use of a random forest-type algorithm with an MAE of 0.37, an RMSE of 0.47, and an R^2 of 0.974. From these bathymetric data, the daily dredging excavation rates were determined. These were $1231.98 \text{ m}^3/\text{day}$ in 2017 and $597.85 \text{ m}^3/\text{day}$ in 2018. The analysis of the bathymetries indicates that, after this dredging, the bottom

recovered almost immediately (in the dredging of 2018 in 5 days) with filling rates of 589.90 and 3556.35 m³/day, for 2017 and 2018, respectively. It also can be stated that the sporadic arrival of sediment above the mean depth also disappeared without external intervention, keeping the mean depth between −3 and −4 m. As a result, it can be concluded that lowering the elevation by dredging does not seem adequate, unless the dredging depth is close to the average elevation that is maintained naturally.

For future work, it might be useful to extend this investigation to other ports. Before determining the need for dredging, it would be useful to know if there is a depth beyond which it is not appropriate to conduct further dredging due to the rate at which sediment returns. The analysis of the behavior of the bottom of the ports in recent years provides valuable information for the planning of maintenance tasks and the knowledge of their behavior in the face of littoral dynamics.

Author Contributions: Conceptualization, V.M.-P. and F.O.-F.; software and validation, V.M.-P.; methodology, M.C.-B.; data curation, V.M.-P.; writing—original draft preparation, M.C.-B.; writing—review and editing, F.O.-F., and V.R.-M. All authors have read and agreed to the published version of the manuscript.

Funding: This work was funded by the Science, Technology and Innovation Plan of the Principality of Asturias (Spain) Ref: FC-GRUPIN-IDI/2018/000225, which is partly funded by the European Regional Development Fund (ERDF).

Institutional Review Board Statement: Not applicable.

Informed Consent Statement: Not applicable.

Acknowledgments: The authors would like to thank the Port Service and Transport Infrastructures of the Principality of Asturias for their collaboration in this work.

Conflicts of Interest: The authors declare there are no conflict of interest.

References

1. Quang Tri, D.; Kandasamy, J.; Cao Don, N. Quantitative Assessment of the Environmental Impacts of Dredging and Dumping Activities at Sea. *Appl. Sci.* **2019**, *9*, 1703. [[CrossRef](#)]
2. Bolam, S.G.; Rees, H.L. Minimizing Impacts of Maintenance Dredged Material Disposal in the Coastal Environment: A Habitat Approach. *Environ. Manag.* **2003**, *32*, 171–188. [[CrossRef](#)]
3. Norén, A.; Fedje, K.K.; Strömvall, A.-M.; Rauch, S.; Andersson-Sköld, Y. Integrated Assessment of Management Strategies for Metal-Contaminated Dredged Sediments—What Are the Best Approaches for Ports, Marinas and Waterways? *Sci. Total Environ.* **2020**, *716*, 135510. [[CrossRef](#)]
4. Wang, W.; Men, C.; Lu, W. Online Prediction Model Based on Support Vector Machine. *Neurocomputing* **2008**, *71*, 550–558. [[CrossRef](#)]
5. Khorram, S.; Khalegh, M.A. A Novel Hybrid MCDM Approach to Evaluate Ports' Dredging Project Criteria Based on Intuitionistic Fuzzy DEMATEL and GOWPA. *WMU J. Marit. Aff.* **2020**, *19*, 95–124. [[CrossRef](#)]
6. Cáceres, R.A.; Zyserman, J.A.; Perillo, G.M.E. Analysis of Sedimentation Problems at the Entrance to Mar Del Plata Harbor. *J. Coast. Res.* **2016**, *32*, 301–314. [[CrossRef](#)]
7. Feola, A.; Lisi, I.; Salmeri, A.; Venti, F.; Pedroncini, A.; Gabellini, M.; Romano, E. Platform of Integrated Tools to Support Environmental Studies and Management of Dredging Activities. *J. Environ. Manag.* **2016**, *166*, 357–373. [[CrossRef](#)]
8. Mahmoodi, A.; Lashteh Neshaei, M.A.; Mansouri, A.; Shafai Bejestan, M. Study of Current- and Wave-Induced Sediment Transport in the Nowshahr Port Entrance Channel by Using Numerical Modeling and Field Measurements. *J. Mar. Sci. Eng.* **2020**, *8*, 284. [[CrossRef](#)]
9. Chen, B.; Wang, K. Suspended Sediment Transport in the Offshore near Yangtze Estuary* *Project Supported by the National Natural Science Foundation of China (Grant No.40576017), the National Basic Research Program of China (973, Program, Grant No. 2007CB411804). *J. Hydrodyn. Ser. B* **2008**, *20*, 373–381. [[CrossRef](#)]
10. Zuo, S.; Xie, H.; Ying, X.; Cui, C.; Huang, Y.; Li, H.; Xie, M. Seabed Deposition and Erosion Change and Influence Factors in the Yangshan Deepwater Port over the Years. *Acta Oceanol. Sin.* **2019**, *38*, 96–106. [[CrossRef](#)]
11. Erftemeijer, P.L.A.; Robin Lewis, R.R. Environmental Impacts of Dredging on Seagrasses: A Review. *Mar. Pollut. Bull.* **2006**, *52*, 1553–1572. [[CrossRef](#)]
12. Flor, G.; del Busto, J.A.; Blanco, G.F. Morphological and Sedimentary Patterns of Ports of the Asturian Region (NW Spain). *J. Coast. Res.* **2006**, *48*, 35–40.

13. Stock, F.; Knipping, M.; Pint, A.; Ladstätter, S.; Delile, H.; Heiss, A.G.; Laermanns, H.; Mitchell, P.D.; Ployer, R.; Steskal, M.; et al. Human Impact on Holocene Sediment Dynamics in the Eastern Mediterranean—the Example of the Roman Harbour of Ephesus. *Earth Surf. Process. Landf.* **2016**, *41*, 980–996. [[CrossRef](#)]
14. Sharaan, M.; Ibrahim, M.G.; Iskander, M.; Masria, A.; Nadaoka, K. Analysis of Sedimentation at the Fishing Harbor Entrance: Case Study of El-Burullus, Egypt. *J. Coast. Conserv.* **2018**, *22*, 1143–1156. [[CrossRef](#)]
15. Poursanidis, D.; Traganos, D.; Reinartz, P.; Chrysoulakis, N. On the Use of Sentinel-2 for Coastal Habitat Mapping and Satellite-Derived Bathymetry Estimation Using Downscaled Coastal Aerosol Band. *Int. J. Appl. Earth Obs. Geoinf.* **2019**, *80*, 58–70. [[CrossRef](#)]
16. Vittori, G.; Blondeaux, P.; Mazzuoli, M.; Simeonov, J.; Calantoni, J. Sediment Transport under Oscillatory Flows. *Int. J. Multiph. Flow* **2020**, *133*, 103454. [[CrossRef](#)]
17. Finn, J.R.; Li, M.; Apte, S.V. Particle Based Modelling and Simulation of Natural Sand Dynamics in the Wave Bottom Boundary Layer. *J. Fluid Mech.* **2016**, *796*, 340–385. [[CrossRef](#)]
18. Finn, J.R.; Li, M. Regimes of Sediment-Turbulence Interaction and Guidelines for Simulating the Multiphase Bottom Boundary Layer. *Int. J. Multiph. Flow* **2016**, *85*, 278–283. [[CrossRef](#)]
19. Kidanemariam, A.G.; Uhlmann, M. Direct Numerical Simulation of Pattern Formation in Subaqueous Sediment. *J. Fluid Mech.* **2014**, *750*, 1–13. [[CrossRef](#)]
20. Leont'yev, I.O.; Akivis, T.M. Modeling of Coastal Dynamics of the Anapa Bay-Bar. *Oceanology* **2020**, *60*, 279–285. [[CrossRef](#)]
21. Armanini, A.; Cavedon, V.; Righetti, M. A Probabilistic/Deterministic Approach for the Prediction of the Sediment Transport Rate. *Adv. Water Resour.* **2015**, *81*, 10–18. [[CrossRef](#)]
22. Flener, C.; Lotsari, E.; Alho, P.; Käyhkö, J. Comparison of Empirical and Theoretical Remote Sensing Based Bathymetry Models in River Environments. *River Res. Appl.* **2012**, *28*, 118–133. [[CrossRef](#)]
23. Giardino, C.; Bresciani, M.; Matta, E.; Brando, V.E. Imaging Spectrometry of Inland Water Quality in Italy Using MIVIS: An Overview. In *Advances in Watershed Science and Assessment*; Younos, T., Parece, T.E., Eds.; Springer International Publishing: Cham, Switzerland, 2015; Volume 33, pp. 61–83. ISBN 978-3-319-14211-1.
24. Jawak, S.D.; Vadlamani, S.S.; Luis, A.J. A Synoptic Review on Deriving Bathymetry Information Using Remote Sensing Technologies: Models, Methods and Comparisons. *Adv. Remote Sens.* **2015**, *4*, 147–162. [[CrossRef](#)]
25. Hedley, J.; Roelfsema, C.; Chollett, I.; Harborne, A.; Heron, S.; Weeks, S.; Skirving, W.; Strong, A.; Eakin, C.; Christensen, T.; et al. Remote Sensing of Coral Reefs for Monitoring and Management: A Review. *Remote Sens.* **2016**, *8*, 118. [[CrossRef](#)]
26. Lyzenga, D.R. Passive Remote Sensing Techniques for Mapping Water Depth and Bottom Features. *Appl. Opt.* **1978**, *17*, 379. [[CrossRef](#)]
27. Cheng, N.-S.; Chiew, Y.-M. Pickup Probability for Sediment Entrainment. *J. Hydraul. Eng.* **1998**, *124*, 232–235. [[CrossRef](#)]
28. Liu, S.; Gao, Y.; Zheng, W.; Li, X. Performance of Two Neural Network Models in Bathymetry. *Remote Sens. Lett.* **2015**, *6*, 321–330. [[CrossRef](#)]
29. El-Mewafi, M.; Salah, M.; Fawzi, B. Assessment of Optical Satellite Images for Bathymetry Estimation in Shallow Areas Using Artificial Neural Network Model. *Am. J. Geogr. Inf. Syst.* **2018**, *7*, 99–106.
30. Obelcz, J.; Wood, W.T.; Phrampus, B.J.; Lee, T.R. Machine Learning Augmented Time-Lapse Bathymetric Surveys: A Case Study from the Mississippi River Delta Front. *Geophys. Res. Lett.* **2020**, *47*, e2020GL087857. [[CrossRef](#)]
31. Tonion, F.; Pirotti, F.; Faina, G.; Paltrinieri, D. A Machine Learning Approach to Multispectral Satellite Derived Bathymetry. *ISPRS Ann. Photogramm. Remote Sens. Spat. Inf. Sci.* **2020**, *3*, 565–570. [[CrossRef](#)]
32. Mavraeidopoulos, A.K.; Oikonomou, E.; Palikaris, A.; Poulos, S. A Hybrid Bio-Optical Transformation for Satellite Bathymetry Modeling Using Sentinel-2 Imagery. *Remote Sens.* **2019**, *11*, 2746. [[CrossRef](#)]
33. Sagawa, T.; Yamashita, Y.; Okumura, T.; Yamanokuchi, T. Satellite Derived Bathymetry Using Machine Learning and Multi-Temporal Satellite Images. *Remote Sens.* **2019**, *11*, 1155. [[CrossRef](#)]
34. Manessa, M.D.M.; Kanno, A.; Sekine, M.; Haidar, M.; Yamamoto, K.; Imai, T.; Higuchi, T. Satellite-Derived Bathymetry Using Random Forest Algorithm and Worldview-2 Imagery. *Geopanning J. Geomat. Plan.* **2016**, *3*, 117–126. [[CrossRef](#)]
35. Kogut, T.; Weistock, M. Classifying Airborne Bathymetry Data Using the Random Forest Algorithm. *Remote Sens. Lett.* **2019**, *10*, 874–882. [[CrossRef](#)]
36. Yunus, A.P.; Dou, J.; Song, X.; Avtar, R. Improved Bathymetric Mapping of Coastal and Lake Environments Using Sentinel-2 and Landsat-8 Images. *Sensors* **2019**, *19*, 2788. [[CrossRef](#)] [[PubMed](#)]
37. Bures, L.; Sychova, P.; Maca, P.; Roub, R.; Marval, S. River Bathymetry Model Based on Floodplain Topography. *Water* **2019**, *11*, 1287. [[CrossRef](#)]
38. Setiawan, K.T.; Suwargana, N.; Ginting, D.N.B.; Manessa, M.D.M.; Anggraini, N.; Adawiah, S.W.; Julzarika, A.; Surahman, S.; Rosid, S.; Supardjo, A.H. Bathymetry extraction from spot 7 satellite imagery using random forest methods. *Int. J. Remote Sens. Earth Sci. IJReSES* **2019**, *16*, 23–30. [[CrossRef](#)]
39. Moeinkhah, A.; Shakiba, A.; Azarakhsh, Z. Assessment of Regression and Classification Methods Using Remote Sensing Technology for Detection of Coastal Depth (Case Study of Bushehr Port and Kharg Island). *J. Indian Soc. Remote Sens.* **2019**, *47*, 1019–1029. [[CrossRef](#)]

40. Ha, N.T.; Manley-Harris, M.; Pham, T.D.; Hawes, I. A Comparative Assessment of Ensemble-Based Machine Learning and Maximum Likelihood Methods for Mapping Seagrass Using Sentinel-2 Imagery in Tauranga Harbor, New Zealand. *Remote Sens.* **2020**, *12*, 355. [[CrossRef](#)]
41. Misra, A.; Ramakrishnan, B. Assessment of Coastal Geomorphological Changes Using Multi-Temporal Satellite-Derived Bathymetry. *Cont. Shelf Res.* **2020**, *207*, 104213. [[CrossRef](#)]
42. Huber, M.E.; Zigic, S.; Gilbert, R.; Smith, D.; Edison, K.; Goudkamp, K.; Langtry, S.; Burling, M. Improved Dredge Material Management for the Great Barrier Reef Region. In Proceedings of the Australasian Port and Harbour Conference; Engineers Australia: Barton, Australia, 2013; p. 400.
43. Lara, J.L.; Lucio, D.; Tomas, A.; Di Paolo, B.; Losada, I.J. High-Resolution Time-Dependent Probabilistic Assessment of the Hydraulic Performance for Historic Coastal Structures: Application to Luarda Breakwater. *Philos. Trans. R. Soc. Math. Phys. Eng. Sci.* **2019**, *377*, 20190016. [[CrossRef](#)]
44. Nalona (Suction Dredger) Registered in—Vessel Details, Current Position and Voyage Information—IMO 9047453 | AIS Marine Traffic. Available online: <https://www.marinetraffic.com> (accessed on 18 September 2019).
45. Sentinel Application Platform. ESA Toolboxes, 2009. SNAP. Available online: <http://step.esa.int/main/toolboxes/snap> (accessed on 12 January 2020).
46. Lanaras, C.; Bioucas-Dias, J.; Galliani, S.; Baltasvias, E.; Schindler, K. Super-Resolution of Sentinel-2 Images: Learning a Globally Applicable Deep Neural Network. *ISPRS J. Photogramm. Remote Sens.* **2018**, *146*, 305–319. [[CrossRef](#)]
47. Rumora, L.; Miler, M.; Medak, D. Impact of Various Atmospheric Corrections on Sentinel-2 Land Cover Classification Accuracy Using Machine Learning Classifiers. *ISPRS Int. J. Geo-Inf.* **2020**, *9*, 277. [[CrossRef](#)]
48. Son, N.-T.; Chen, C.-F.; Chen, C.-R.; Guo, H.-Y. Classification of Multitemporal Sentinel-2 Data for Field-Level Monitoring of Rice Cropping Practices in Taiwan. *Adv. Space Res.* **2020**, *65*, 1910–1921. [[CrossRef](#)]
49. Alwhaely, U.; Hussein, M.A.; AL-Kaaby, L.F. Using GIS and Remote Sensing Satellite Data to Mapping and Monitoring Shatt Al-Arab Estuary (out Bar Area) and Nearby Coastline Southern Iraq. *Al-Qadisiyah J. Pure Sci.* **2020**, *25*, 1–21. [[CrossRef](#)]
50. Breiman, L. Random Forests. *Mach. Learn.* **2001**, *45*, 5–32. [[CrossRef](#)]
51. Reiss, H.; Cunze, S.; König, K.; Neumann, H.; Kröncke, I. Species Distribution Modelling of Marine Benthos: A North Sea Case Study. *Mar. Ecol. Prog. Ser.* **2011**, *442*, 71–86. [[CrossRef](#)]
52. James, G.; Witten, D.; Hastie, T.; Tibshirani, R. *An Introduction to Statistical Learning*; Springer: Cham, Switzerland, 2013; Volume 112.
53. Prasad, A.M.; Iverson, L.R.; Liaw, A. Newer Classification and Regression Tree Techniques: Bagging and Random Forests for Ecological Prediction. *Ecosystems* **2006**, *9*, 181–199. [[CrossRef](#)]
54. Peters, J.; Baets, B.D.; Verhoest, N.E.C.; Samson, R.; Degroeve, S.; Becker, P.D.; Huybrechts, W. Random Forests as a Tool for Ecohydrological Distribution Modelling. *Ecol. Model.* **2007**, *207*, 304–318. [[CrossRef](#)]
55. Kuhn, M. Caret: Classification and Regression Training. R Package Version. Available online: <https://www.R-project.org> (accessed on 5 February 2021).
56. Mateo-Pérez, V.; Corral-Bobadilla, M.; Ortega-Fernández, F.; Vergara-González, E.P. Port Bathymetry Mapping Using Support Vector Machine Technique and Sentinel-2 Satellite Imagery. *Remote Sens.* **2020**, *12*, 2069. [[CrossRef](#)]
57. Confederación Hidrográfica del Cantábrico. Available online: <https://www.chcantabrico.es/las-cuencas-cantabricas/marco-fisico/hidrologia/rios/negro> (accessed on 12 November 2019).